

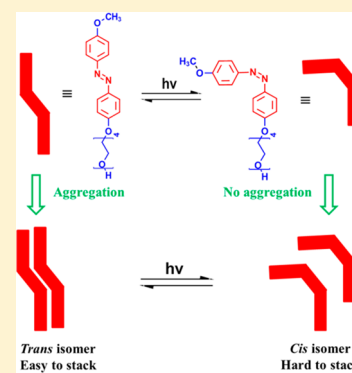
Conformation of Novel Azo-Dyes Bearing End-Capped Oligo(ethylene glycol) Studied by UV–vis and NMR Spectroscopy

Cassandre Kouvas,[†] Wilms E. Baille,[†] Jesús Ortiz-Palacios,[‡] Edgar Aguilar-Ortíz,[‡] Ernesto Rivera,^{*,‡} and X. X. Zhu^{*,†}

[†]Département de chimie, Université de Montréal, C.P. 6128, Succursale Centre-ville, Montréal, Québec H3C 3J7, Canada

[‡]Instituto de Investigaciones en Materiales, Universidad Nacional Autónoma de México, Circuito Exterior Ciudad Universitaria, C.P. 04510 México D.F., México

ABSTRACT: Two novel azo-dyes bearing an end-capped oligo(ethylene glycol) chain were synthesized and then studied by UV–visible and NMR spectroscopy. For both azobenzenes, the end-capped oligo(ethylene glycol) segment is on the para position of the first phenyl ring. On the second phenyl ring, a methoxy group is added on the para position for one azo-dye and no substitution group on the other, which made them electronically a push–push and a push system, respectively. The presence of the methoxy group changes significantly the absorption and the photoisomerization behaviors and results in a much less intense absorbance for the trans isomer and a shift from 350 to 360 nm. In the kinetic studies the azobenzene bearing a methoxy group shows a zero-order and a first-order kinetics as a function of the time scale of the study as well as an aggregation phenomenon. This azo-dye in different solvents has been studied by ¹H NMR and pulsed gradient NMR experiments to understand the effects of the photoisomerization and the aggregation on the self-diffusion of these molecules in solutions.



INTRODUCTION

Azobenzene molecules, initially used as dyes, have been widely studied due to their reversible isomerization properties. The light-induced isomerization of the azo dye *N*-ethyl-*N*-(2-hydroxyethyl)-4-(4-nitrophenylazo)aniline (Disperse Red 1) grafted onto thin polymer films was first reported by two research groups.^{1,2} Azobenzenes can switch from the trans (*E*) to cis (*Z*) isomers when they are irradiated preferably with linear polarized light at the appropriate wavelength. Their photochromic behavior makes them potential molecular switches due to the photoinduced motions.^{3,4} Polymers may be made to be light-responsive after the incorporation or grafting of azo dyes.^{2,5,6} The substitution groups on azo-dyes have a significant influence on the absorption spectra and the formation of H or J aggregates.⁷ The position and the shape of the characteristic bands $\pi\text{--}\pi^*$ (more intense for the trans isomer) and $n\text{--}\pi^*$ (more intense for the cis isomer)^{3,7,8} strongly depend on the nature of the substitution groups. Figure 1 shows a typical absorption spectrum for azobenzene molecules with two main bands, a $\pi\text{--}\pi^*$ transition at 350 nm and another $n\text{--}\pi^*$ transition at 450 nm. If the azobenzene unit is substituted by an electron-donor group (R_1) and an electron-withdrawing group (R_2), known as “push–pull” systems,³ a red shift of the $\pi\text{--}\pi^*$ band and a blue shift of the $n\text{--}\pi^*$ band are observed.

The incorporation of hydrophilic or amphiphilic polymer chains into azo-dyes can induce their micellization in water.^{9–11} The photochemical behavior of such polymeric materials may be studied by UV–vis spectroscopy and by pulsed field gradient (PFG) NMR techniques.¹² PFG NMR has been used to study

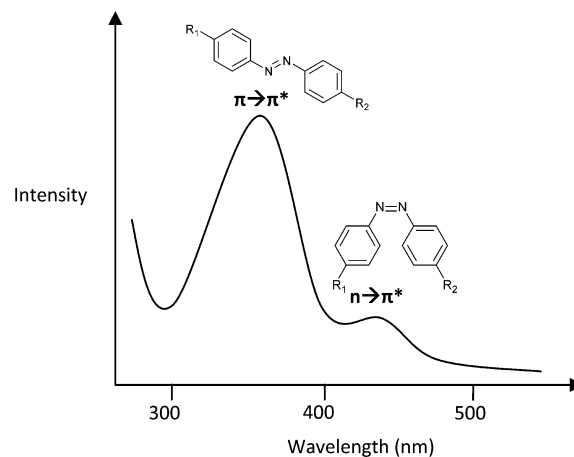


Figure 1. UV–vis absorption spectrum of a para-substituted azobenzene.

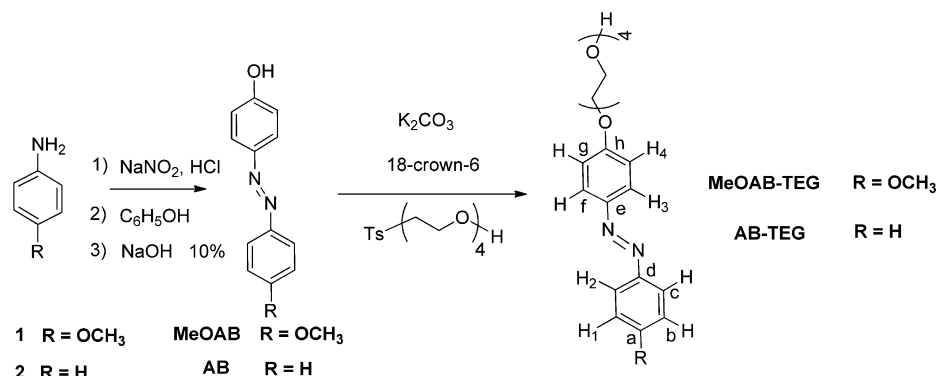
diffusion of small molecules in polymers systems such as modified polysaccharides,^{13–15} and self-diffusion of linear, star, and dendritic poly(ethylene glycol)s in water¹⁶ and in hydrogels.^{17,18} The self-diffusion behavior of the azo-dyes in different media may provide additional information on the intermolecular interaction and aggregation depending on the

Received: June 18, 2015

Revised: August 24, 2015

Published: August 24, 2015

Scheme 1



molecular configuration (trans or cis) and the substitution groups.

Herein, we synthesized two azobenzene derivatives bearing a TEG segment on the para position of the first phenyl ring and a similar azo-dye bearing a methoxy group on the para position of the other phenyl ring, which made them a push system and a push–push system, respectively. First, UV–vis spectroscopy was used to characterize these molecules in aqueous media and their cis-to-trans thermal relaxation kinetics. Then, PFG NMR experiments were done with the azo-dyes dissolved in different solvents before irradiation after trans-to-cis and after cis-to-trans photoisomerizations to study the self-diffusion and the dynamics of the azobenzene units.

EXPERIMENTAL SECTION

Synthesis. All reagents used in the synthesis of the azobenzenes were purchased from Aldrich and used as received. The syntheses of the azobenzenes bearing a tetra(ethylene glycol) (TEG) segment are shown in Scheme 1. The diazonium salts of the two azobenzenes were prepared in situ because these salts are not commercially available. Precursor Ts-TEG was synthesized according to a method previously reported.¹⁹

Synthesis of the 4-Methoxy-4'-tetraethylene Glycol-azobenzene (MeOAB-TEG). *p*-Anisidine **1** (1 g, 8.13 mmol) and NaNO₂ (0.56 g, 8.13 mmol) were dissolved in a HCl aqueous solution (30%, 50 mL) at 0 °C with vigorous stirring. Then, phenol (0.764 g, 8.13 mmol) was added to the solution and was stirred for 1 h at room temperature. Afterward, the reaction mixture was neutralized with a NaOH solution (10%) and stirred for 3 h. The product was filtered and dried to a constant weight to yield azo-compound MeOAB. Yield: 75%.

The intermediate Ts-TEG (0.72 g, 2.19 mmol) was reacted with MeOAB (0.5 g, 2.19 mmol), K₂CO₃ (1.21 g, 8.77 mmol), and a catalytic amount of 18-crown-6 in dry acetone (25 mL). The reaction mixture was heated to reflux for 48 h; then, it was cooled to room temperature, filtered, and concentrated at reduced pressure. The crude product was purified by column chromatography on silica gel using a mixture of ethyl acetate/hexane 9:1 and pure ethyl acetate as eluent, to give the azobenzene derivative MeOAB-TEG. Yield: 90%. ¹H NMR (400 MHz, CDCl₃) (Scheme 1): δ = 7.83 (d, *J* = 8.7 Hz, 2 H, H²), 7.82 (d, *J* = 8.7 Hz, 2 H, H³), 6.97 (d, *J* = 8.5 Hz, 2 H, H⁴), 6.95 (d, *J* = 8.0 Hz, 2 H, H¹), 4.18 (t, *J* = 4.25 Hz, 2 H, PhN=NPhOCH₂), 3.84 (s, 3H, PhOCH₃), 3.11–3.55 (m, 14 H, OCH₂ of the tetra(ethylene glycol) chain). ¹³C NMR (100 MHz, CDCl₃) (Scheme 1): δ = 161.36 (1C, C^h), 160.55 (1C, C^a), 146.90 (1C, C^d), 146.80 (1C, C^e), 124.12 (2C, C^c), 124.07

(2C, C^f), 114.58 (2C, C^b), 113.94 (2C, C^g), 72.32 (1C, HOCH₂CH₂), 70.61–70.11 (4C, OCH₂ of the tetra(ethylene glycol) chain), 69.42 (1C, PhN=NPhOCH₂CH₂), 67.46 (PhN=NPhOCH₂), 61.45 (1C, HOCH₂CH₂), 55.32 (1C, PhOCH₃).

Synthesis of the 4'-Tetra(ethylene glycol)-azobenzene (AB-TEG). The same synthetic procedure (replacing *p*-anisidine **1** by aniline **2**) was used for the synthesis of 1-hydroxyazobenzene with a yield of 85%. Then, Ts-TEG (0.83 g, 2.52 mmol) was reacted with 1-hydroxyazobenzene (0.5 g, 2.52 mmol) by using the same procedure as previously described for the synthesis of MeOAB-TEG to give the desired azo-compound AB-TEG. Yield: 92%. ¹H NMR (400 MHz, CDCl₃) (Scheme 1): δ = 7.90 (d, *J* = 8.9 Hz, 2 H, H²), 7.86 (d, *J* = 7.75 Hz, 2 H, H³), 7.51–7.41 (m, 3 H, H¹), 7.03 (d, *J* = 8.96 Hz, 2 H, H⁴), 4.22 (t, *J* = 4.6 Hz, 2H, PhN=NPhOCH₂), 3.89 (t, *J* = 4.92 Hz, 2 H, PhN=NPhOCH₂CH₂), 3.75–3.60 (m, 12 H, OCH₂ of the tetra(ethylene glycol) chain). ¹³C NMR (100 MHz, CDCl₃) (Scheme 1): δ = 160.94 (1C, C^h), 152.33 (1C, C^d), 146.65 (1C, C^e), 130.07 (1C, C^a), 128.69 (2C, C^b), 124.39 (2C, C^f), 122.23 (2C, C^c), 113.48 (2C, C^g), 72.21 (1C, HOCH₂CH₂), 70.41–69.91 (4C, OCH₂ of the tetra(ethylene glycol) chain), 69.20 (1C, PhN=NPhOCH₂CH₂), 67.33 (1C, PhN=NPhOCH₂CH₂), 61.21 (1C, HOCH₂CH₂).

Samples Irradiation. Absorption spectra were acquired on an OmniCure S2000 Spot UV Curing System. The UV light for irradiation was generated by a high-pressure 200 W mercury vapor short arc UV lamp. The azobenzene photoisomerization experiments were performed in 20 mL glass bottles. To obtain light sources in the range of desired wavelengths, we introduced 320–390 and 400–500 nm filters successively into the light guide for the trans-to-cis and the cis-to-trans isomerization, respectively.^{8,19,20}

Absorption Spectroscopy. The kinetics of relaxation were studied after the trans-to-cis and cis-to-trans photoisomerization for both azobenzenes in water solutions.²¹ Samples for absorption spectroscopy measurements were prepared in distilled water, with an azo-compound concentration of 0.04 and 0.20 mg/mL for AB-TEG and MeOAB-TEG, respectively. The absorption spectra were recorded in 1 cm quartz cells on a Cary 5000 UV–vis-NIR spectrophotometer at room temperature.

NMR Experiments. ¹H and ¹³C NMR spectra of the compounds in CDCl₃ were recorded at room temperature on a Bruker Avance 400 spectrometer operating at 400 and 100 MHz for ¹H and ¹³C nuclei, respectively. The ¹H PFG NMR experiments were performed at 25 °C using 5 mm anti-UV

NMR tubes on the same NMR spectrometer equipped with an ultrastable temperature controller and also with a Diff 60 diffusion probe, a 5 mm autotuning broad-band probe with a z-gradient coil permitting a maximum gradient of 3000 G/cm. For self-diffusion experiments, 6 mg of the azobenzene sample was dissolved in 1 mL of a deuterated solvent such as D₂O (99.9 atom % ²H), CD₃OD (99.8 atom % ²H), and DMSO-*d*₆ (99.9 atom % ²H), all purchased from Sigma-Aldrich.

A stimulated echo pulse sequence (STE: 90-*t*₁-90-*t*₂-90-*t*₁-echo)¹⁶ was used for the NMR experiments. The self-diffusion coefficients of the azobenzenes in different solvents were determined according to the following equation

$$I = I_0 e^{-D(\gamma\delta G)^2 \left(\Delta - \frac{\delta}{3} \right)} \quad (1)$$

where I_0 and I are the NMR signals in the absence and in the presence of the gradient pulses, respectively, D is the self-diffusion coefficient in the Z direction, γ is the gyromagnetic ratio of the observed nucleus ($\gamma_{\text{H}} = 2.67522128 \times 10^7 \text{ rad T}^{-1} \text{ s}^{-1}$), δ is the gradient length, G is the gradient strength, and Δ is the time interval between two gradient pulses.^{22,23} The self-diffusion coefficients D were calculated with a coefficient of determination (R^2) in the range of 0.98 to 0.99.

RESULTS AND DISCUSSION

Absorption Spectroscopy. Prior to the irradiation study, the UV-vis spectrum of each azobenzene is obtained to determine the wavelength of excitation, which mainly depends on the nature of the substitution groups. The spectra in Figure 2

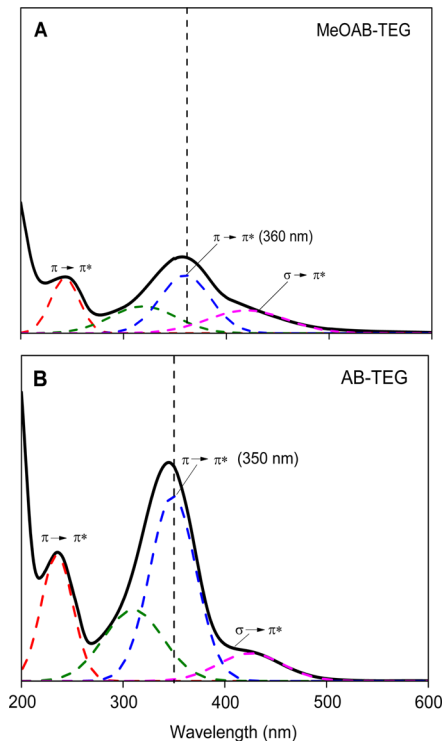


Figure 2. UV-vis spectra of (A) MeOAB-TEG (0.04 mg/mL) and (B) AB-TEG (0.20 mg/mL) and their deconvolution spectra (dashed spectra) before irradiation. A red shift of the trans band from 350 to 360 nm is observed when the azobenzene is para-substituted with an electron-donor group, as shown by the vertical dashes in panels A and B.

show three main absorption bands for both MeOAB-TEG and AB-TEG in water: The first two strong bands at 240 and 350 nm are assigned to the $\pi \rightarrow \pi^*$ transition, which are associated with the transition dipole moments along the short and long axis of the azobenzene molecules, respectively.²⁴ Only the band at 350 nm was used to characterize both MeOAB-TEG and AB-TEG molecules because the trans-to-cis isomerization is promoted by irradiation with wavelengths between 320 and 390 nm (using a filter). The third band corresponding to $n \rightarrow \pi^*$ transition at 420 nm (forbidden transition) represents the cis isomer.

The deconvoluted absorption spectra of both azobenzenes exhibit four characteristic bands (Figures 2A,B). The trans isomer is more stable at the equilibrium than the cis and is the dominant species. In fact, the $\pi \rightarrow \pi^*$ band intensity is higher than the $n \rightarrow \pi^*$ band in each spectrum because the latter transition is not allowed according to the symmetry rules.⁴ The AB-TEG spectrum shows a much intense $\pi \rightarrow \pi^*$ band than MeOAB-TEG, even though AB-TEG is five times less concentrated than MeOAB-TEG. Therefore, the molar absorption coefficient of AB-TEG should be substantially higher than that of MeOAB-TEG. Furthermore, the absorption band $\pi \rightarrow \pi^*$ shifts from 350 to 360 nm (Figure 2, vertical dashes) when a methoxy group is added to the phenyl ring. This is due to the electron-donor nature of this substituent, which red-shifts the $\pi \rightarrow \pi^*$ band. The effect would have been even more pronounced if an electron-withdrawing group had been attached in the place of TEG because a push-pull system instead of a push-push system would have induced a stronger red shift of the $\pi \rightarrow \pi^*$ absorption band, thereby causing a total overlap with the absorption $n \rightarrow \pi^*$ band.^{3,4}

Photoisomerization. The aqueous solutions of AB-TEG and MeOAB-TEG were irradiated for 15 min at 320–390 nm for the trans-to-cis and at 400–500 nm for the cis-to-trans isomerizations (Figure 3). In the spectra of AB-TEG, a significant decrease in intensity of the $\pi \rightarrow \pi^*$ band (from 75.8 to 11.3) is observed after irradiation for the trans-to-cis isomerization (Figure 3A and Table 1), while the irradiation of the cis isomer induces an increased intensity of the same band (Figure 3A), but the $\pi \rightarrow \pi^*$ band area (55.3) does not recover its original value (75.8) before irradiation (Table 1). The area may be fully recovered through cis-to-trans thermal relaxation, with the complete formation of the trans isomer.³ The $n \rightarrow \pi^*$ band has a small change in intensity during the trans-to-cis isomerization, increasing from 16.6 to 22.0 (Table 1), but it is not considered to be significant because this absorption band does not correspond to an allowed transition.

The spectra of MeOAB-TEG show a different behavior after the trans-to-cis isomerization. The intensities of the trans and cis bands both increase (Figure 3B). The area under the trans isomer band rises from 32.3 to 44.0 (Table 1) in contrast with the decrease in the $\pi \rightarrow \pi^*$ absorption band due to the trans-to-cis transformation of AB-TEG. The area under the $n \rightarrow \pi^*$ band also rises by almost three-fold from 13.5 to 52.0, much larger than the increase for the trans-to-cis isomerization of AB-TEG (Table 1). The $\pi \rightarrow \pi^*$ band intensity further increases after the cis-to-trans isomerization (Figure 3B), and the area increases from 44.0 to 114.4, about 3.5 times higher than the initial value (32.3) (Table 1). Once again, this is very different from the 73% recovery obtained for AB-TEG. These changes in the adsorption spectra are typically related to the packing of trans isomers. The methoxy group added on the phenyl ring induces the formation of aggregates when MeOAB-TEG is in

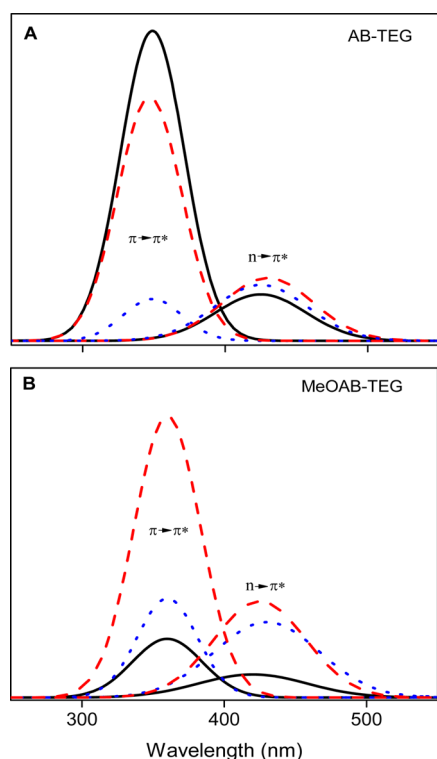


Figure 3. Deconvoluted UV-vis spectra for (A) AB-TEG and (B) MeOAB-TEG. Solid lines, before the trans-to-cis irradiation; blue dots, after the trans-cis irradiation at 320–390 nm; red dashes, after the cis-to-trans irradiation at 400–500 nm. The peaks close to 350 nm are the $\pi \rightarrow \pi^*$ band, while the ones close to 430 nm correspond to the $n \rightarrow \pi^*$ band. For MeOAB-TEG, the $\pi \rightarrow \pi^*$ band after the cis-to-trans irradiation (red dashes) will decrease with time due to the aggregation of the azo-dye, while AB-TEG does not show this aggregation process.

its trans form. Usually this behavior results from intermolecular hydrophilic, hydrophobic, van der Waals interactions, and hydrogen bonding.^{7,9,24–26} The planar (E) conformation of the azo groups allows the molecules to interact with each other by van der Waals forces through the phenyl ring and by hydrogen bonds between the methoxy group and the TEG chain.^{7,26}

At the equilibrium state, the MeOAB-TEG molecules tend to stack, forming H-aggregates before the trans-to-cis isomerization. (A hypsochromic shift is observed when azobenzenes aggregate under the influence of a solvent, an additive, or a change in concentration.)^{7,10,26} When the molecules are irradiated at 320–390 nm, the aggregates may break up under the heat generated by the irradiation as a function of time (total of 15 min for all measurements), thus releasing free MeOAB-TEG molecules, which are instantly isomerized to the cis form. The cis isomer has a bent structure,³ hindering the packing and the interaction between these molecules and

promoting the disaggregation and the dissolution of azo-dyes.^{9,24,27,28} The irradiation liberates individual trans isomers from the aggregates and thus induces an increase in the $n \rightarrow \pi^*$ band intensity (Figure 3B) because more single trans isomers are available for the trans-to-cis isomerization.

The intensity of the $\pi \rightarrow \pi^*$ band is higher after the irradiation at 400–500 nm (Figure 3B) than at the initial equilibrium because the proportion of single trans isomers is higher after cis-to-trans photoisomerization due to the delay in forming the aggregates. These results are further confirmed by the NMR experiments.

Kinetics. AB-TEG and MeOAB-TEG in water were irradiated for 15 min at 320–390 nm for the trans-to-cis isomerization. The absorption spectra were recorded every hour to study the kinetics of cis-to-trans thermal relaxation, which can be qualitatively evaluated by the apparent extent of photoisomerization Y_{app} ²⁵

$$Y_{app}(t) = \frac{I_{trans}(0) - I_{trans}(t)}{I_{trans}(0)} \quad (2)$$

where $I_{trans}(0)$ and $I_{trans}(t)$ are the intensities of the trans absorption band at 349 nm before (assuming all azo-dyes are in the trans form) and after irradiation at 320–390 nm at time t , respectively. In addition, this thermal relaxation can be described by the ratio of isomerization R_i , that is, the mole fraction of trans form of the azo-dyes²⁵

$$R_i(t) = \frac{I_{trans}(0) - I_{trans}(t)}{I_{trans}(0) - I_{trans}(\infty)} \quad (3)$$

where $I_{trans}(0)$, $I_{trans}(t)$, and $I_{trans}(\infty)$ are the intensities of the absorption band at 349 nm (more intense for the trans) before (assuming all azo-dyes are in the trans form) and after irradiation at 320–390 nm at time t and at infinity, respectively.

Figure 4A,B shows the evolution of Y_{app} and $1 - R_i$ with time after irradiation of AB-TEG at 320–390 nm. A first order for the cis-to-trans thermal relaxation is observed, as described by eqs 4 and 5^{25,29}

$$Y_{app}(t) = Y_{app}(0) - kt \quad (4)$$

$$1 - R_i(t) = 1 - \frac{kt}{I_{trans}(0) - I_{trans}(\infty)} \quad (5)$$

where $Y_{app}(0)$ and $Y_{app}(t)$ are the apparent extents of photoisomerization at the photostationary state and at time t , respectively, and k represent the rate constant for the thermal cis-to-trans isomerization. The half lives $t_{1/2}$ for the two approaches can be expressed by^{30,31}

$$t_{1/2} = \frac{Y_{app}(0)}{2k} \quad (6)$$

Table 1. Position and Area of trans and cis Absorption Bands of AB-TEG and MeOAB-TEG before and after the trans-to-cis and the cis-to-trans Isomerization

transitions	MeOAB-TEG isomer				AB-TEG isomer			
	$\pi \rightarrow \pi^*$		$n \rightarrow \pi^*$		$\pi \rightarrow \pi^*$		$n \rightarrow \pi^*$	
	λ_{max} (nm)	area	λ_{max} (nm)	area	λ_{max} (nm)	area	λ_{max} (nm)	area
before irradiation	361	32.3	428	13.5	350	75.8	425	16.6
trans→cis 320–390 nm	361	44.0	436	52.0	345	11.3	432	22.0
cis→trans 400–500 nm	361	114.4	428	57.5	350	55.3	433	16.6

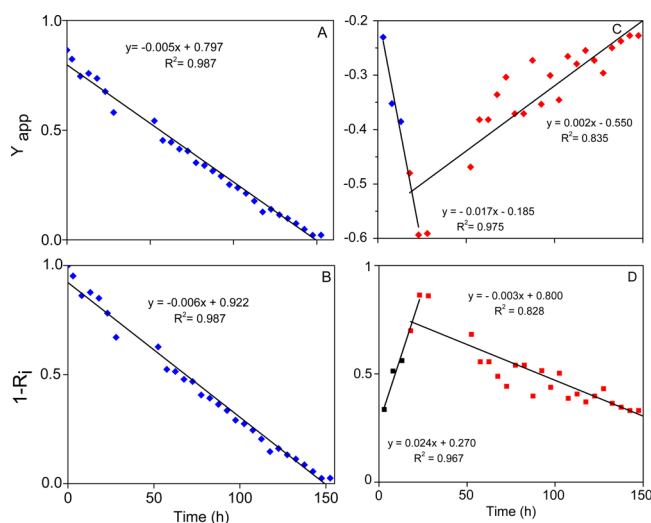


Figure 4. Evolution of the values of Y_{app} (A and C, fits to eq 4) and $1 - R_i$ (B and D, eq 5) with time for AB-TEG (A,B) and MeOAB-TEG (C,D) in water.

$$t_{1/2} = \frac{I_{\text{trans}}(0) - I_{\text{trans}}(\infty)}{2k} \quad (7)$$

Table 2 lists the characteristic constants of the cis-to-trans thermal relaxation of AB-TEG for these two methods, and both lead to similar rate constants k and half lives $t_{1/2}$.

For MeOAB-TEG, the thermal cis-to-trans relaxation has two stages. The first 30 h are dominated by the cis-to-trans isomerization, which was determined as a zero-order reaction (Figures 4C,D). Another trend stands out after 50 h and globally appears to have first-order kinetics. It is actually composed of two reactions, a cis-to-trans isomerization and the aggregation of the individual trans isomers. If both reactions are described by zero-order kinetics the rate coefficient and the half-life time can be extracted from $k = k_{\text{cis} \rightarrow \text{trans}} - k_{\text{aggr}}$ in eq 8 (Table 2).³² The velocity of the competition (V_{comp}) between the aggregation and the cis-to-trans relaxation can be expressed by

$$V_{\text{comp}} = kY_{\text{app}} = (k_{\text{cis} \rightarrow \text{trans}} - k_{\text{aggr}})Y_{\text{app}} \quad (8)$$

where $k_{\text{cis} \rightarrow \text{trans}}$, k_{aggr} , and k are the rate constants of pure cis-to-trans relaxation, aggregation and the combination of the relaxation and aggregation for MeOAB-TEG, respectively.

If we consider both reactions as zero-order reactions, $k_{\text{cis} \rightarrow \text{trans}}$ for MeOAB-TEG is 3 times higher than that of AB-TEG (Tables 1 and 2). Thus, the relaxation of MeOAB-TEG is faster. The half life for the thermal relaxation of MeOAB-TEG is 5.43 h until aggregation appears, which induces a competition between these two processes. Furthermore, the rate constant of the pure cis-to-trans relaxation is higher than that of the

aggregation, which means that the latter is the rate-limiting reaction. The isomerization from *cis*- to *trans*-MeOAB-TEG is faster than the packing of the freshly isomerized trans isomers. This could explain the higher proportion of trans isomers at the end of the relaxation compared with the initial value.

NMR Diffusion Experiments. For a better understanding of the aggregation of MeOAB-TEG in the trans form, we studied the self-diffusion of MeOAB-TEG in three different solvents by ^1H PGSE NMR experiments. The experiments were done on MeOAB-TEG in D_2O and in $\text{DMSO}-d_6$ before and after 15 min of irradiation at 320–390 and at 400–500 nm. In CD_3OD the irradiation was limited to 5 min because methanol is more volatile. The spectra in Figure 5 show different peaks for the trans and cis isomers in the three solvents used. Thus, the characteristic peaks for each isomer were chosen to calculate the self-diffusion coefficients presented in Table 3. (Aromatic peaks are used due to overlapping peaks from the aliphatic part of the cis and trans isomers.) The solubilities of trans and cis isomers in D_2O are different. Figure 5A shows that MeOAB-TEG is not detectable before irradiation; after irradiation at 320–390 nm, however, the cis isomer is detectable and remains visible even after irradiation at 400–500 nm (cis to trans isomerization). In Figure 5B,C, the trans and cis isomers are visible both before and after irradiation at 320–390 and at 400–500 nm, respectively.

The aromatic peaks of both azobenzenes were used to determine the self-diffusion coefficients because the peaks of the aliphatic parts of the cis and trans isomers have overlapping signals. The self-diffusion coefficients of MeOAB-TEG determined in the different deuterated solvents are shown in Table 3. Because a very low percentage of cis isomers exist at the equilibrium or before irradiation (Figure 5) the measurement of the self-diffusion coefficient for this isomer is not precise in $\text{DMSO}-d_6$ and CD_3OD . The azobenzene molecules are mainly in their trans conformation before the irradiation. The van der Waals interactions between the azo-dyes are stronger because the trans isomers are more stretched, which induces the packing of molecules so that the solubility was too low to be detected by NMR (Figure 5A, before irradiation). MeOAB-TEG becomes soluble in D_2O after the trans-to-cis irradiation because the cis isomers have a bent structure and cannot pack as easily and therefore have a slightly higher solubility, which allowed the calculation of the self-diffusion coefficient of the cis isomer ($3.79 \times 10^{-10} \text{ m}^2/\text{s}$, Table 3).

In $\text{DMSO}-d_6$, MeOAB-TEG is more soluble. Before irradiation, the D_{cis} and D_{trans} values of MeOAB-TEG are similar ($(2.19$ and $2.15) \times 10^{-10} \text{ m}^2/\text{s}$, respectively). After irradiation at 320–390 nm a more significant difference in D values of the two isomers is observed ($(2.19$ and $1.97) \times 10^{-10} \text{ m}^2/\text{s}$ for cis and trans isomers, respectively). In this case, MeOAB-TEG exists mainly in the cis conformation, and aggregated trans isomers are dissociated. After irradiation at

Table 2. Determination of Zero-Order Rate Constant k and Half Life $t_{1/2}$ with the Y_{app} and R_i Methods for MeOAB-TEG and MeOAB-TEG in Water

	AB-TEG		MeOAB-TEG					
			pure cis-to-trans relaxation		aggregation and cis-to-trans relaxation		aggregation	
	k (h^{-1})	$t_{1/2}$ (h)	$k_{\text{cis} \rightarrow \text{trans}}$ (h^{-1})	$t_{1/2}$ (h)	k (h^{-1})	$t_{1/2}$ (h)	k_{agg} (h^{-1})	$t_{1/2 \text{agg}}$ (h)
with Y_{app} eq 4	5.3×10^{-3}	75.3	1.71×10^{-2}	5.4	2.3×10^{-3}	119.6	1.48×10^{-2}	18.6
with R_i eq 5	6.2×10^{-3}	74.4	2.49×10^{-2}	5.4	3.4×10^{-2}	117.8	2.15×10^{-2}	18.9

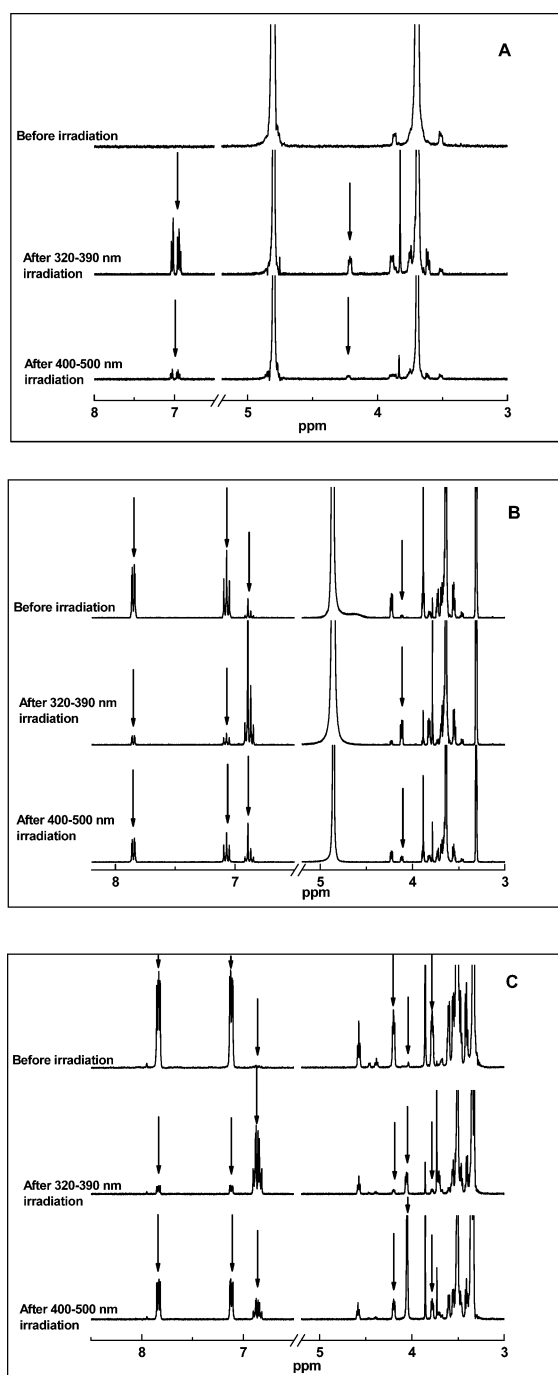


Figure 5. ^1H NMR spectra of MeOAB-TEG in D_2O (A), CD_3OD (B), and $\text{DMSO}-d_6$ (C) before and after irradiations at 320–390 and 400–500 nm, respectively. The intensities of these peaks were used to determine the self-diffusion coefficients.

400–500 nm, however, the D values of the two isomers become similar again.

Both trans and cis isomers are soluble in CD_3OD . The higher self-diffusion coefficient values obtained in CD_3OD (generally over 3 times higher in value, Table 3) are mainly due to the higher solubility and the lower viscosity of the solution in comparison with $\text{DMSO}-d_6$ and D_2O solutions. Right after irradiation at 400–500 nm, the trans isomers are not yet aggregated and behave similarly as the cis isomers, and a small percentage of the cis isomers still remains (Table 1). Therefore, the D_{cis} of MeOAB-TEG is higher in D_2O than in $\text{DMSO}-d_6$. The packing in D_2O occurs in a few hours, as shown in a kinetic study.

CONCLUSIONS

The azobenzene derivatives bearing an end-capped oligo-(ethylene glycol) show a very different absorption behavior when a methoxy group was added to the phenyl ring at the para position of the TEG group. In fact, the intensity obtained for the 1-methoxy-azobenzene is much lower than its non-methoxylated counterpart, even though its concentration is 5 times higher. Therefore, the molar absorption coefficient of AB-TEG is substantially higher than that of MeOAB-TEG. Both molecules exhibit trans-to-cis and cis-to-trans transitions when they are irradiated at 320–390 nm and then at 400–500 nm, respectively. After the cis-to-trans photoisomerization, the azobenzene bearing a methoxy group tends to stack, forming H aggregates. The formation of aggregates after cis-to-trans isomerization leads to a decreased absorbance as a function of time.

The study of cis-to-trans thermal relaxation shows that the presence of the methoxy group changes significantly the relaxation process. For example, AB-TEG shows a first-order reaction with the two methods, one based on the apparent extent of photoisomerization and the other on isomerization ratio. In contrast, two trends were observed in the case of MeOAB-TEG: a first-order process during the first 30 h and another first-order trend starting around 50 h; however, the spectral change observed indicates that the preferential cis-to-trans isomerization of both azobenzene proceeds spontaneously at room temperature, even without light irradiation. Furthermore, the rate constant determined for MeOAB-TEG is faster than AB-TEG, which leads to a shorter half life for MeOAB-TEG.

The PFG NMR experiments did not show any significant difference in the self-diffusion coefficients for AB-TEG and MeOAB-TEG. The D values vary in the different solvents, and important differences were observed before and after irradiation due to the disruption of the aggregation through irradiation and the slow kinetics of the aggregation of the trans isomers.

Table 3. Self-Diffusion Coefficients for MeOAB-TEG in Various Solvents before and after Irradiation

solvent	D_{cis} (10^{-10} m ² /s)			D_{trans} (10^{-10} m ² /s)		
	before irradiation	after irradiation		before irradiation	after irradiation	
		320–390 nm	400–500 nm		320–390 nm	400–500 nm
D_2O	N/A	3.79	3.68	N/A	N/A	N/A
CD_3OD	7.22	7.14	7.26	7.17	7.32	6.85
$\text{DMSO}-d_6$	2.19	2.15	2.12	2.15	1.97	2.16

■ AUTHOR INFORMATION

Corresponding Authors

*E.R.: E-mail: riverage@unam.mx.

*X.X.Z.: E-mail: julian.zhu@umontreal.ca.

Notes

The authors declare no competing financial interest.

■ ACKNOWLEDGMENTS

DGAPA-UNAM (PAPIIT IN100513) and NSERC of Canada are acknowledged for financial support. We also thank Mr. Sylvain Essiembre and Dr. Cedric Malveau for their help in selected experiments.

■ REFERENCES

- (1) Rochon, P.; Batalla, E.; Natansohn, A. Optically induced surface gratings on azoaromatic polymer films. *Appl. Phys. Lett.* **1995**, *66*, 136–138.
- (2) Kim, D. Y.; Tripathy, S. K.; Li, L.; Kumar, J. Laser-induced holographic surface relief gratings on nonlinear optical polymer films. *Appl. Phys. Lett.* **1995**, *66*, 1166–1168.
- (3) Beharry, A. A.; Woolley, G. A. Azobenzene photoswitches for biomolecules. *Chem. Soc. Rev.* **2011**, *40*, 4422–4437.
- (4) Merino, E.; Ribagorda, M. Control over molecular motion using the cis-trans photoisomerization of the azo group. *Beilstein J. Org. Chem.* **2012**, *8*, 1071–1090.
- (5) Gelover-Santiago, A.; Fowler, M. A.; Yip, J.; Duhamel, J.; Burillo, G.; Rivera, E. Unexpected absorbance enhancement upon clustering dyes in a polymer matrix. *J. Phys. Chem. B* **2012**, *116*, 6203–6214.
- (6) Intawiat, N.; Pettersen, M. K.; Rukke, E. O.; Meier, M. A.; Vogt, G.; Dahl, A. V.; Skaret, J.; Keller, D.; Wold, J. P. Effect of different colored filters on photooxidation in pasteurized milk. *J. Dairy Sci.* **2010**, *93*, 1372–1382.
- (7) Rivera, E.; Carreón-Castro, M.; Buendia, I.; Cedillo, G. Optical properties and aggregation of novel azo-dyes bearing an end-capped oligo(ethylene glycol) side chain in solution, solid state and Langmuir–Blodgett films. *Dyes Pigm.* **2006**, *68*, 217–226. Han, R. M.; Hara, M. Chain length-dependent photoinduced formation of azobenzene aggregates. *New J. Chem.* **2006**, *30*, 223–227.
- (8) Rivera, E.; Carreón-Castro, M. d. P.; Salazar, R.; Huerta, G.; Becerril, C.; Rivera, L. Preparation and characterization of novel grafted polyethylene based azo-polymers bearing oligo(ethylene glycol) spacers. *Polymer* **2007**, *48*, 3420–3428.
- (9) Rijcken, C. J.; Soga, O.; Hennink, W. E.; van Nostrum, C. F. Triggered destabilisation of polymeric micelles and vesicles by changing polymers polarity: an attractive tool for drug delivery. *J. Controlled Release* **2007**, *120*, 131–148.
- (10) Caicedo, C.; Rivera, E.; Valdez-Hernández, Y.; Carreón-Castro, M. d. P. Synthesis and characterization of novel liquid-crystalline azo-dyes bearing two amino-nitro substituted azobenzene units and a well-defined, oligo(ethylene glycol) spacer. *Mater. Chem. Phys.* **2011**, *130*, 471–480.
- (11) Song, B.; Hu, Y.; Song, Y.; Zhao, J. Alkyl chain length-dependent viscoelastic properties in aqueous wormlike micellar solutions of anionic gemini surfactants with an azobenzene spacer. *J. Colloid Interface Sci.* **2010**, *341*, 94–100.
- (12) Inglesby, M. K.; Zeronian, S. H. Diffusion coefficients for direct dyes in aqueous and polar aprotic solvents by the NMR pulsed-field gradient technique. *Dyes Pigm.* **2001**, *50*, 3–11.
- (13) Thérien-Aubin, H.; Zhu, X. X. NMR spectroscopy and imaging studies of pharmaceutical tablets made of starch. *Carbohydr. Polym.* **2009**, *75*, 369–379.
- (14) Thérien-Aubin, H.; Baille, W. E.; Zhu, X. X.; Marchessault, R. H. Imaging of high-amylose starch tablets. 3. Initial diffusion and temperature effects. *Biomacromolecules* **2005**, *6*, 3367–3372.
- (15) Wang, Y. J.; Ravenelle, F.; Zhu, X. X. NMR imaging study of cross-linked high-amylose starch tablets: The effect of drug loading. *Can. J. Chem.* **2010**, *88*, 202–207.
- (16) Wang, Y. J.; Thérien-Aubin, H.; Baille, W. E.; Luo, J. T.; Zhu, X. X. Effect of molecular architecture on the self-diffusion of polymers in aqueous systems: A comparison of linear, star, and dendritic poly(ethylene glycol)s. *Polymer* **2010**, *51*, 2345–2350.
- (17) Thérien-Aubin, H.; Zhu, X. X.; Moorefield, C. N.; Kotta, K.; Newkome, G. R. Effect of Ionic Binding on the Self-Diffusion of Anionic Dendrimers and Hydrophilic Polymers in Aqueous Systems as Studied by Pulsed Gradient NMR Techniques. *Macromolecules* **2007**, *40*, 3644–3649.
- (18) Thérien-Aubin, H.; Baille, W. E.; Zhu, X. X. Diffusion of molecular probes and the effects of their interactions with polymer matrices as studied by pulsed-field gradient NMR spectroscopy. *Can. J. Chem.* **2008**, *86*, 579–585.
- (19) Rivera, E.; Belletête, M.; Natansohn, A.; Durocher, G. Synthesis, characterization, and optical properties of a novel azo-dye bearing an oligo(ethylene glycol) methyl ether side chain in solution and in the solid state. *Can. J. Chem.* **2003**, *81*, 1076–1082.
- (20) Liu, R.; Xiao, Q.; Li, Y.; Chen, H.; Yan, Z.; Zhu, H. Phenyleneethynyleneazobenzenes with symmetrical peripheral chromophores: Synthesis, optical properties and photoisomerization behaviors study. *Dyes Pigm.* **2012**, *92*, 626–632.
- (21) Liu, J.; Zhang, Q.; Zhang, J. Synthesis and characterization of photochromic star-like liquid crystal. *Mater. Lett.* **2005**, *59*, 2531–2534.
- (22) Nicolay, K.; Braun, K. P.; Graaf, R. A.; Dijkhuizen, R. M.; Kruskamp, M. J. Diffusion NMR spectroscopy. *NMR Biomed.* **2001**, *14*, 94–111.
- (23) Walderhaug, H.; Soderman, O.; Topgaard, D. Self-diffusion in polymer systems studied by magnetic field-gradient spin-echo NMR methods. *Prog. Nucl. Magn. Reson. Spectrosc.* **2010**, *56*, 406–425.
- (24) Kajiyama, T.; Aizawa, M. *New Developments in Construction and Functions of Organic Thin Films*; Elsevier: New York, 1996.
- (25) Takahashi, M.; Okuhara, T.; Yokohari, T.; Kobayashi, K. Effect of packing on orientation and cis-trans isomerization of azobenzene-chromophore in Langmuir–Blodgett film. *J. Colloid Interface Sci.* **2006**, *296*, 212–219.
- (26) Rivera, E.; Carreón-Castro, M. d. P.; Rodríguez, L.; Cedillo, G.; Fomine, S.; Morales-Saavedra, O. G. Amphiphilic azo-dyes (RED-PEGM). Part 2: Charge transfer complexes, preparation of Langmuir–Blodgett films and optical properties. *Dyes Pigm.* **2007**, *74*, 396–403.
- (27) Narayan, G.; Kumar, N. S. S.; Paul, S.; Srinivas, O.; Jayaraman, N.; Das, S. Aggregation and photoresponsive behavior of azobenzene-oligomethylene-glucopyranosidebolaamphiphiles. *J. Photochem. Photobiol., A* **2007**, *189*, 405–413.
- (28) Freyer, W.; Brete, D.; Schmidt, R.; Gahl, C.; Carley, R.; Weinelt, M. Switching behavior and optical absorbance of azobenzene-functionalized alkanethiols in different environments. *J. Photochem. Photobiol., A* **2009**, *204*, 102–109.
- (29) Haro, M.; Villares, A.; Gascón, I.; Martín, S.; Oriol, L.; Cea, P. Photochemical behaviour of an acid-terminated azopolymer in solution and in Langmuir–Blodgett films. *Curr. Appl. Phys.* **2010**, *10*, 874–879.
- (30) Tait, K. M.; Parkinson, J. A.; Bates, S. P.; Ebenezer, W. J.; Jones, A. C. The novel use of NMR spectroscopy with in situ laser irradiation to study azophotoisomerisation. *J. Photochem. Photobiol., A* **2003**, *154*, 179–188.
- (31) Sarkar, N.; Sarkar, A.; Sivaram, S. Isomerization behavior of aromatic azo chromophores bound to semicrystalline polymer films. *J. Appl. Polym. Sci.* **2001**, *81*, 2923–2928.
- (32) Garcia-Amorós, J.; Sanchez-Ferrer, A.; Massad, W. A.; Nonell, S.; Velasco, D. Kinetic study of the fast thermal cis-to-trans isomerisation of para-,ortho- and polyhydroxyazobenzenes. *Phys. Chem. Chem. Phys.* **2010**, *12*, 13238–13242.